Morphological Control of Periodic Mesoporous Organosilica with Agitation

Sung Soo Park, Chi Hun Lee, Jong Hyeon Cheon, Sang Joon Choe, and Dong Ho Park*

Department of Chemistry, Inje University, Kyungnam, Kimhae 621-749, Korea
Received March 19, 2001

Periodic mesoporous organosilicas with rope-based morphology from a reaction gel composition of 1 BTME : 0.57 ODTMABr : 2.36 NaOH : 353 H_2O were synthesized. While long rope-shaped product dominated in case of static synthesis condition, gyroid type products instead of rope shaped product appeared and rope shaped product disappeared with agitation. PMO with such a long rope shaped morphology is firstly reported. Additionally, various rope-based morphologies depending on the degree of bending, twisting, folding and winding of rope such as spirals, discoids, toroids, and worm-like aggregates were observed. White powdered products were characterized by X-ray diffraction, N_2 sorption measurement, SEM and TEM. From XRD pattern and TEM image, ODTMA-PMO with hexagonal symmetry was identified. The pore diameter and BET surface area of ODTMA-PMO are 32.9 Å and 799 m^2g^{-1}, respectively. Hexagonally arrayed channels run with long axis of rope and rope-based shapes with various degree of curvature, which was elucidated by using TEM images.

Keywords : Morphological control, Periodic mesoporous organosilica, Agitation, Long rope, Gyroid.

Introduction

Surfactant-mediated synthesis method for mesoporous materials, which was initiated by Mobil group,[1,2] made it possible to the formation of periodic mesoporous organosilicas (PMO).[3-7] These organic-inorganic hybrid materials contain covalently-linked organic group in the mesoporous framework and have a narrow pore size distribution in the range of 20 to 40 Å. Three groups, by which PMO was independently synthesized, pointed out that it is possible to embed directly metal center in the wall, mediate the framework polarity, and control the hardness and density of mesophase. The organic functionalization of framework opens up the possibility for many applications such as sensing, enantioselective separation, asymmetric syntheses, chromatographic supports and so on. It is apparent that the morphology control as well as handling and texture of mesoporous silicas is extremely important for many applications.[8-29] Recently the mesoporous silica with morphologies including fibers, thin films, monoliths, hexagonal prisms, toroids, discoids, spirals, dodecahedron, and hollow tubular shapes have been synthesized.[15,16,26,28,30-33] From a series of papers by Ozin group,[28,29,34,35] it was suggested that curved morphologies of mesoporous silica depend on a specific kind of dislocation or disclination defect with a rotation vector along the six-fold (C_6, $\pm \pi/3$), three fold (C_3, $\pm 2\pi/3$), two-fold (C_2, $\pm \pi$), (v_1, or v_2, $+ \pi$ or $+ 2\pi$) axes as shown in Figure 1, which initiates growth and determines form in a germinating and polymerizing silicate mesophase.

Herein we describe the synthesis of periodic mesoporous organosilicas with long rope shape and a variety of rope-based morphologies depending on the degree of bending, folding and/or winding such as multiple winding rope, spirals, toroids, discoids, and worm-like aggregates. And We considered the effect on the morphology of agitation in the course of reaction. We as well as Sayari group adopted the preparation procedure reported by Inagakis group, except of using CTABr instead of CTACl as a structure-directing agent in this study. We have concentrated the preparation and formation mechanism of long rope-shaped morphology and the morphological control with agitation, as compared with Sayaris report. PMO with such a long rope-shaped morphology is firstly reported. Comparing to inorganic mesoporous silicate material, the morphogenesis for hybrid organic-inorganic mesoprous materials have been rarely reported.[36,37]

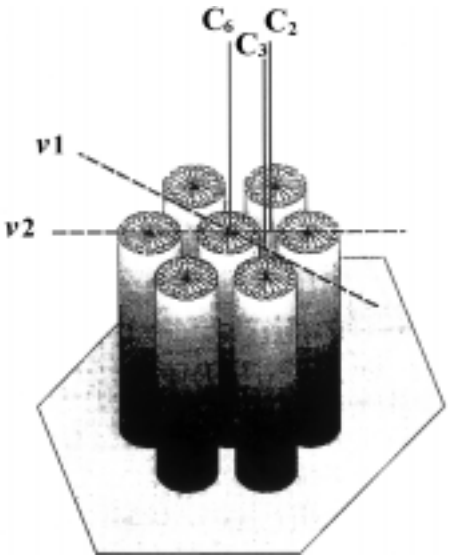

Figure 1. Illustration of symmetry elements in a rod-like 2D hexagonal array that are relevant to the structure of topological defects.

*To whom correspondence should be addressed. Tel: +82-55-334-2073; Fax: +82-55-321-9718; e-mail: chempdh@ijnc.inje.ac.kr

Experimental Section

Synthesis of ODTMA-PMO. We have applied the procedure described by Inagaki group to prepare hybrid organic-inorganic mesoporous materials.[3]

Octadecyltrimethylammonium bromide (ODTMABr) was first dissolved in water with stirring at 60 °C to obtain a clear solution. NaOH was then added to the ODTMABr solution with stirring. The mixture was transferred to a teflon bottle, and 1,2-bis(trimethoxysilyl)ethane (BTME) added drop by drop to the solution under vigorous stirring and mild heating. After being stirred for 12 h at room temperature, the clear solution was sealed in Teflon-lined autoclave and was kept at 95 °C for 6 h. The stirring temperature and reaction duration was changed in order to investigate the variation of morphology. The molar composition of the mixture was 1 BTME : 0.57 ODTMABr : 2.36 NaOH : 353 H_2O. The white product was collected by filtration, washed with deionized water, and dried at 60 °C, which is designated by ODTMA-PMO.

The surfactant was removed by solvent extraction process as followed. 1 g of sample was stirred in 150 ml of water with 3 ml of 37 wt % HCl at 60 °C for 6 h, and the resulting solids were recovered by filtration, washed with ethanol, and dried at 60 °C. The remaining surfactants were removed by repeating this process.

Octadecyltrimethylammonium bromide (ODTMABr, from Aldrich) as a structure-directing surfactant and 1,2-bis(trimethoxysilyl)ethane (BTME, from Aldrich, 96%) as a precursor for periodic mesoporous organosilica were used. Sodium hydroxide (from Yakuri Co. Ltd, > 99%), and absolute ethanol (from Hayman, 99.9% v/v) were purchased. All chemicals were used as purchased.

Characterization. X-ray powder diffraction (XRD) patterns were obtained by Rigaku D/Max 2200 diffractometer using a Cu Kα radiation of wavelength 1.5406 Å. The adsorption and desorption isotherm of nitrogen at −196 °C was measured using Micromeritics ASAP2010 instrument. The sample was pretreated at 200 °C. The pore size distribution curve was obtained from an analysis of desorption branch of the isotherm by using Barrett-Joyner-Halenda (BJH) method. Scanning electron microscopy (SEM) images were obtained using a KEVEX Sigma microscope with an acceleration voltage of 20 kV. The samples were coated with gold using a HITACHI E-1010 sputter coater prior to imaging. Transmission electron microscopy (TEM) images were obtained using a JEOL JEM-2010 microscope operating at 200 kV.

Results and Discussion

The pH of the initial reaction mixture was about 13, and that of the resulting mixture decreased to about 12 after hydrothermal treatment at 95 °C for 6 h, which is indicative of the formation of siloxane bridge between BTMEs through hydrolysis of methoxide to hydroxide followed by condensation. We confirmed that the solvent extraction to remove the surfactants did not affect the morphology.

Figure 2 shows the XRD pattern of surfactant-extracted ODTMA-PMO. The XRD pattern shows three resolved diffraction peaks that can be indexed to the (100), (110), and (200) reflections of a hexagonal symmetry lattice. It indicates that ODTMA-PMO has a *p6mm* hexagonal mesostructure analogous to an ordered mesoporous MCM-41, as reported in other literatures.[1,2] The hexagonal lattice parameter, a_o, calculated from 2θ value of (100) peak was 54.3 Å. Well-resolved XRD peaks reflect a highly structural order extended over a long range, which is consistent with the result of the TEM image as shown in Figure 4. Nitrogen adsorption and desorption isotherms show a type-IV isotherm, as shown in Figure 3, indicating that this material had uniform mesopores

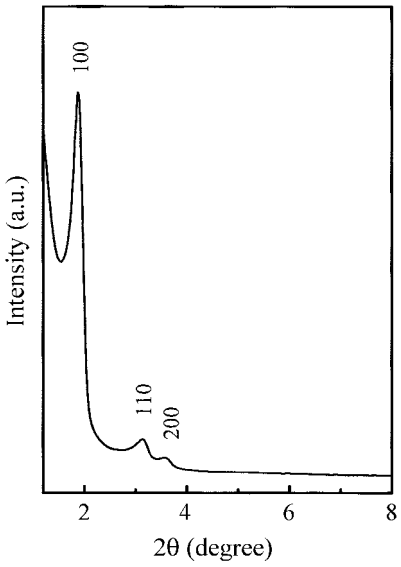

Figure 2. X-ray diffraction pattern of surfactant-extracted ODTMA-PMO.

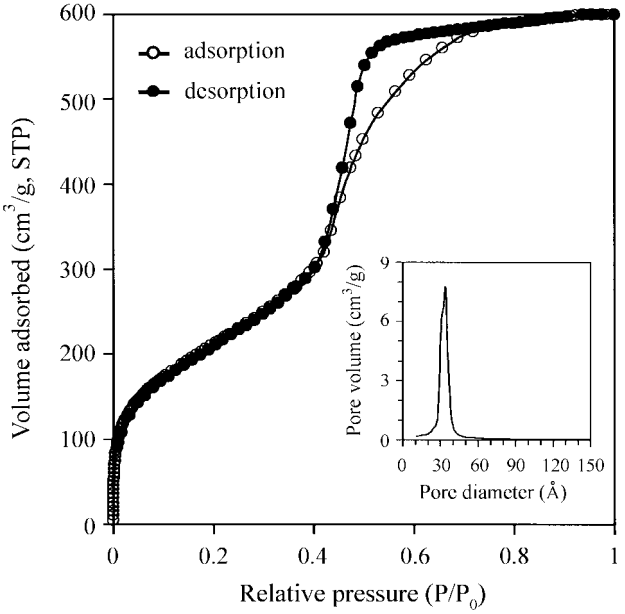

Figure 3. N_2 adsorption-desorption isotherm for surfactant-extracted ODTMA-PMO. Inset shows the pore size distribution obtained using desorption branch by BJH method.

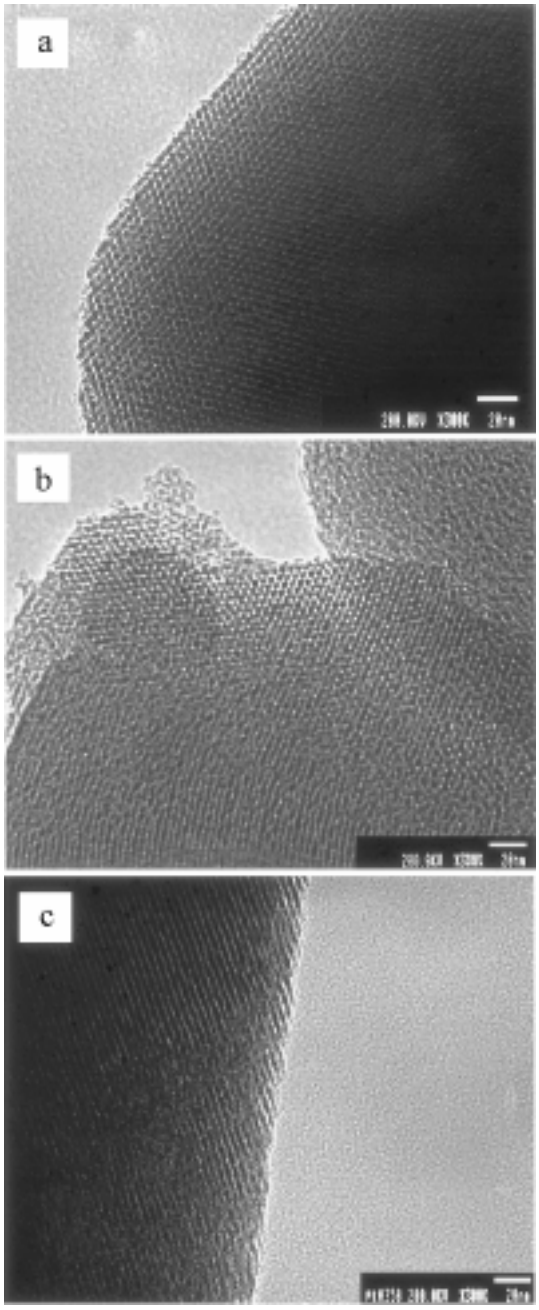

Figure 4. TEM images for (a) hexagonal basal plane, (b) faceted bending part, and (c) twisted part of surfactant-extracted ODTMA-PMO with rope shaped morphology, respectively.

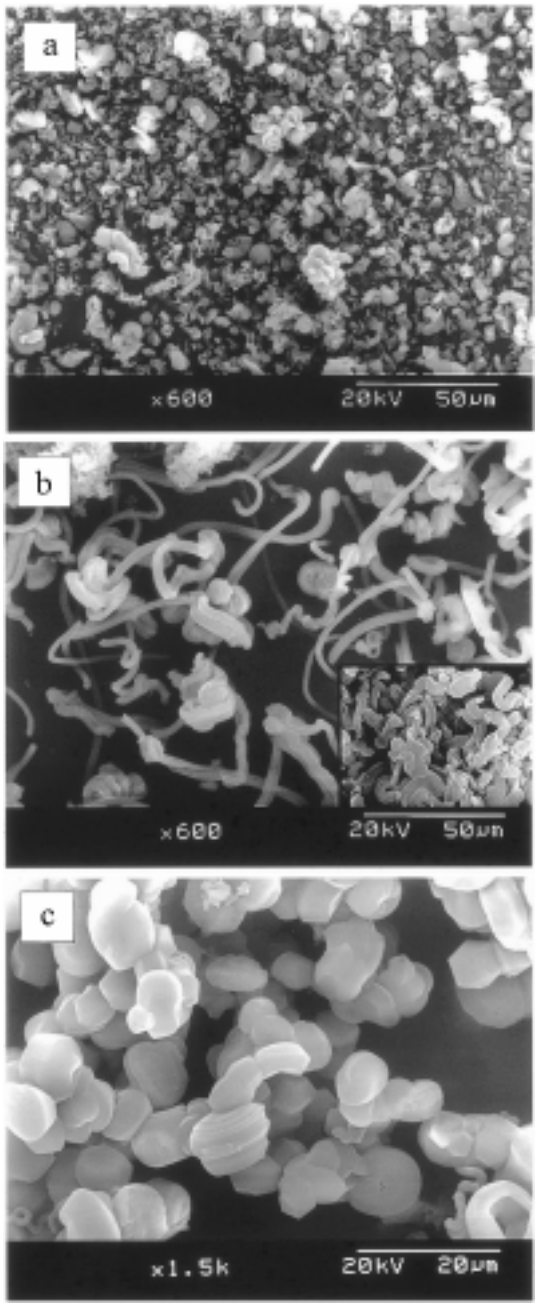

Figure 5. SEM images of surfactant-extracted ODTMA-PMO synthesized at 95 °C for (a) 21 h without agitation after stirring at 60 °C, (b) 6 h without agitation after stirring at room temperature and (c) 21 h with agitation after stirring at room temperature. Inset shows a worm-like aggregate.

with pore diameter of 32.9 Å calculated by BJH method. And BET surface area was 799 $m^2 g^{-1}$.

Figure 4 shows the TEM image of surfactant-extracted ODTMA-PMO. The hexagonal arrayed mesopores with a center-to-center spacing of ~50 Å are ordered well, as shown in Figure 4(a). The TEM images show domains on the hexagonal basal plane of the hexagonal rope (Figure 4(a)) and the faceted bending parts that run down the hexagonal rope (Figure 4(b)).

Figure 5(a) and (b) show SEM images of ODTMA-PMO synthesized at 95 °C for (a) 21 h without agitation after stirring at 60 °C, (b) 6 h without agitation after stirring at room temparuture and (c) 21 h with agitation after stirring at room temperature, respectively. When synthesized at 95 °C for 21 h after stirring at 65 °C, long rope-shaped product does not generate, although broken short rods and small rope aggregates and single particulates such as spirals and gyroids etc. are found. When synthesized at 95 °C for 6 h under static condition, rope-shaped product dominates and worm-like shaped aggregates are rarely present as shown in Figure 5(b). Inset in Figure 5(b) shows SEM image of a worm-like aggregate. Such a long hexagonal rope shaped mesoporous

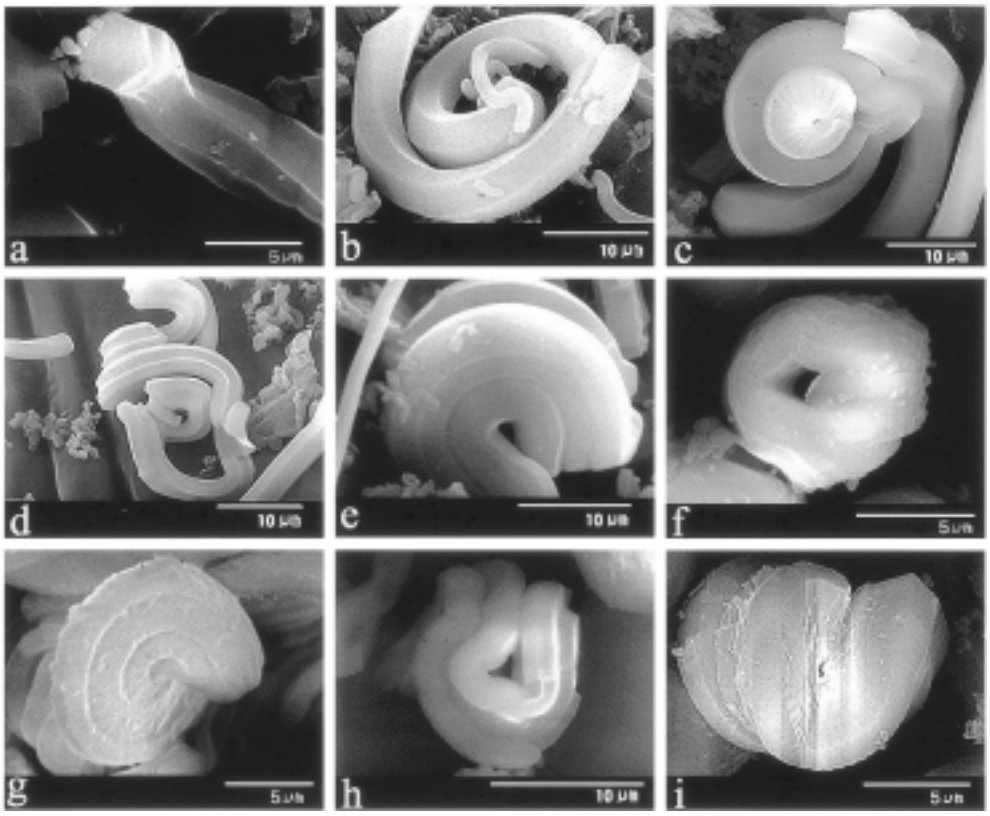

Figure 6. SEM images of surfactant-extracted ODTMA-PMO with various rope-based morphologies.

silicate material have been rarely observed,[9,26,38,39] and PMO is firstly reported. In addition, SEM images of ODTMA-PMO synthesized in a reaction batch display various remarkable shapes based on rope in a batch, as shown in Figure 6. The rope shaped morphology with low curvature disappears dramatically, while most of products exhibit a diversity of morphologies with a high curvature, as shown in Figure 5(c). It may be attributed to sustain an identical regional environment in reaction batch and favor side-to-side growth of rod and seed with decrease of surface double layer charge density by agitation. Agitation of reaction mixture in the course of reaction prohibits rope from lengthening in the direction of c-axis through end-to-end growth between seed and hexagonal micellar rod.

Ozin group suggested that morphologies of mesoporous silicate MCM-41 depend largely on the degree of curvature and the accretion type induced by various topological defects in a hexagonal silicate liquid crystal seed in directing the growth of hexagonal mesoporous silica toward specific morphology.[28,29,35] Complex structure based on combined defects can lead to a variety of mesoporous morphologies. It could be adopted to interpret remarkable morphologies of periodic mesoporous organosilica, although wall property of periodic mesoporous organosilica distinguishes from that of mesoporous silica MCM-41 due to organic moiety within framework.

The hexagonal rope in Figure 6(a) has a twisted and curved body and a hexagonal faceted surface along longitudinal axis of rope with a thickness of *ca*. 3 μm. And TEM image of hexagonal basal plane, as shown in Figure 4(a), shows a well-ordered hexagonal array, while parallel curved surface channels run down the body length of the rope, as shown in Figure 4(b). These imply that the hexagonal ropes may extend in size by accretion of surfactant-organosilica micelles on the basal plane. And the terminal part sometimes exhibits the dislocation of hexagonal platelet that seems to be a building unit of rope, as shown in Figure 6(a). The degree of dislocation seems to depend on the degree of rope curvature, the thickness of stacking platelet and the degree of attraction force between hexagonal faces of neighboring platelet. Higher van der Waals attraction and lower surface double layer repulsion between hexagonal faces of unit due to lower surface charge density of organic-inorganic hybrid framework compared with inorganic analogue could possibly promote the growth of hexagonal rope toward c-axis of hexagonal unit. With increasing the degree of curvature of rope, periodic mesoporous organosilicas with morphology of spirals, toroids, discoids, and worm-like aggregates based on rope are exhibited.

Assuming that the packing geometry of flexible rod-like micelle in the organosilicate liquid crystal seed is hexagonal, the formation of mesoporous organosilica with various rope-based shapes could be partly explained using some kind of dislocation or disclination defects pertinent to the organosilicate liquid crystal seed.

Figure 6(a) shows a part of bent and twisted rope. Bending of rope may be initiated from a disclination rotated along the transverse axis and twisting feature may be resulted from a disclination around the longitudinal axis C_6. While the

parallel curved surface channels of faceted bending parts of hexagonal rope run down the body length of the rope (Figure 4(b)), the surface channels of twisted part run parallel on the tilt from the longitudinal axis of rope (Figure 4(c)). It indicated that disclination about the transverse axes alter the pore orientation, while disclinations about the longitudinal axes alter the rotational configuration of the array. Figure 6(b) exhibits spiral shape emerged from a + 2π disclination along the transverse axis of slightly twisted single rope. Another spiral shaped rope around disk-like core is shown in Figure 6(c). Winding a duplex of rope with various curvature may be initiated from + 2π and + π disclination along the transverse axis (Figure 6(d)). Figure 6(e) exhibits spiral of a triplex of rope induced from + π disclination rotated along the transverse axis. The morphologies such as toroid (Figure 6(f)) and discoid (Figure 6(g)) may be initiated from a + 2π disclination rotated along the transverse axis in the ab-plane and single point spirals from different extents of a + 2π screw dislocation. Complex structures based upon a combination of two defects can lead to a variety of mesoporous morphologies (Figure 6(h) and (i)).

Conclusions

When synthesized at 95 ^{o}C for 6 h under static condition after stirring at room temperature for 12 h, ODTMA-PMO with rope and rope-based shapes dominates. Gyroid type products instead of rope shaped product appeared and rope shaped product disappeared with agitation. PMO with such a long rope shaped morphology is firstly reported. The generation of rope-based morphologies could be interpreted partly in terms of the degree of curvature and the accretion type induced by various topological defects.

Acknowledgment. This study was supported by the academic research fund (BK21, HEKSIM D0024) of Ministry of Education, Republic of Korea.

References

1. Kresge, C. T.; Reonowicz, M. E.; Roth, W. J.; Vartuli, J. C.; Beck, J. S. *Nature* **1992**, *359*, 710.
2. Beck, J. S.; Vartuli, J. C.; Roth, W. J.; Reonowicz, M. E.; Cresge, C. T.; Schmitt, K. D.; Chu, C. T.-W.; Olson, D. H.; Sheppard, E. W.; McCullen, S. B.; Higgins, J. B.; Schlenker, J. L. *J. Am. Chem. Soc.* **1992**, *114*, 10834.
3. Inagaki, S.; Guan, S.; Fukushima, Y.; Ohsuna, T.; Terasaki, O. *J. Am. Chem. Soc.* **1999**, *121*, 9611.
4. Asefa, T.; MacLachlan, M. J.; Coombs, N.; Ozin, G. A. *Nature* **1999**, *402*, 867.
5. Melde, B. J.; Holland, B. T.; Blanford, C. F.; Stein, A. *Chem. Mater.* **1999**, *11*, 3302.
6. Asefa, T.; MacLachlan, M. J.; Grondley, H.; Coombs, N.; Ozin, G. A. *Angew. Chem. Int. Ed. Engl.* **2000**, *39*, 1808.
7. Yoshina-Ishii, C.; Asefa, T.; Coombs, N.; MacLachlan, M. J.; Ozin, G. A. *Chem. Commun*. **1999**, 2539.
8. Lee, T.; Yao, N.; Aksay, I. A. *Langmuir* **1997**, *13*, 3866.
9. Schächt, S.; Huo, Q.; Voigt-Martin, I. G.; Stucky, G. D.; Schüth, F. *Science* **1996**, *273*, 768.
10. Aksay, I. A.; Trau, M.; Manne, S.; Honma, I.; Yao, N.; Zhou, L.; Fenter, P.; Eisenberger, P. M.; Gruner, S. M. *Science* **1996**, *273*, 892.
11. Zhao, D.; Huo, Q.; Feng, J.; Chmelka, B. F.; Stucky, G. D. *J. Am. Chem. Soc*. **1998**, *120*, 6024.
12. Zhao, D.; Feng, J.; Huo, Q.; Melosh, N.; Fredrickson, N.; Chmelka, B. F.; Stucky, G. D. *Science* **1998**, *279*, 548.
13. Davis, S. A.; Burkett, S. L.; Mendelson, N. H.; Mann, S. *Nature* **1997**, *385*, 420.
14. Mann, S.; Ozin, G. A. *Nature* **1996**, *382*, 313.
15. Trau, M.; Yao, N.; Kim, E.; Xia, Y.; Whitesides, G. A.; Aksay, I. A. *Nature* **1997**, *390*, 674.
16. Yang, H.; Coombs, N.; Ozin, G. A. *Adv. Mater.* **1997**, *9*, 811.
17. Tanev, P. T.; Liang, Y.; Pinnavaia, T. J. *J. Am. Chem. Soc*. **1997**, *119*, 8616.
18. Tanev, P. T.; Pinnavaia, T. J. *Science* **1996**, *271*, 1267.
19. Tolbert, S. H.; Schäffer, T. E.; Feng, J.; Hansma, P. K.; Stucky, G. D. *Chem. Mater.* **1997**, *9*, 1962.
20. Sokolov, I.; Yang, H.; Ozin, G. A.; Kresge, C. T. *Adv. Mater.* **1999**, *11*, 636.
21. Huo, Q.; Zhao, D.; Feng, J.; Weston, K.; Buratto, S. K.; Stucky, G. D.; Schacht, S.; Schüth, F. *Adv. Mater.* **1997**, *9*, 974.
22. Yang, P.; Deng, T.; Zhao, D.; Feng, P.; Pine, D. J.; Chmelka, B. F.; Whitesides, G. M.; Stucky, G. D. *Science* **1998**, *282*, 2244.
23. Kim, S. S.; Zhang, W.; Pinnavaia, T. J. *Science* **1998**, *282*, 1302.
24. Huo, Q.; Feng, J.; Schüth, F.; Stucky, G. D. *Chem. Mater.* **1997**, *9*, 14.
25. Yang, S. M.; Yang, H.; Coombs, N.; Sokolov, I.; Kresge, C. T.; Ozin, G. A. *Adv. Mater.* **1999**, *11*, 52.
26. Bruinsma, P. J.; Kim, A. Y.; Liu, J.; Baskaran, S. *Chem. Mater.* **1997**, *9*, 2507.
27. Yang, P.; Zhao, D.; Chmelka, B. F.; Stucky, G. D. *Chem. Mater.* **1998**, *10*, 2033.
28. Yang, H.; Coombs, N.; Ozin, G. A. *Nature* **1997**, *386*, 692.
29. Ozin, G. A.; Yang, H.; Sokolov, I.; Coombs, N. *Adv. Mater.* **1997**, *9*, 662.
30. Kim, J. M.; Kim, S. K.; Ryoo, R. *Chem. Commun*. **1998**, 259.
31. Oliver, S.; Kuperman, A.; Coombs, N.; Lough, A.; Ozin, G. A. *Nature* **1995**, *378*, 47.
32. Zhu, G.; Qiu, S.; Yu, J.; Gao, F.; Xiao, F.; Xu, R.; Sakamoto, Y.; Terasaki, O. In *Proceedings of the 12th International Zeolite Conference*; Treacy, M. M. J., Markus, B. K., Bisher, M. E., Higgins, J. B., Eds.; MRS: Warrendale, 1998; pp 1863-1870.
33. Lin, H. P.; Mou, C. Y. *Science* **1996**, *273*, 765.
34. Yang, H.; Ozin, G. A.; Kresge, C. T. *Adv. Mater.* **1998**, *10*, 883.
35. Ozin, G. A.; Kresge, C. T.; Yang, H. In *Mesoporous Molecular Sieve 1998, Studies in Surface Science and Catalysis, Vol. 117*; Bonneviot, L., Béland, F., Danumah, C., Giasson, S., Kaliaguine, S., Eds.; Elsevier: Amsterdam, 1988; pp 119-127.
36. Guan, S.; Inagaki, S.; Oshuna, T.; Terasaki, O. *J. Am. Chem. Soc*. **2000**, *122*, 5660.
37. Sayari, A.; Hamoudi, S.; Yang, Y.; Moudrakovski, I. L.; Ripmeester, J. R. *Chem. Mater.* **2000**, *12*, 3857.
38. Zhao, D.; Sun, J.; Li, Q.; Stucky, G. D. *Chem. Mater.* **2000**, *12*, 275.
39. Schulz-Ekloff, G.; Rathousky, J.; Zukal, A. *Microporous and Mesoporous Materials* **1999**, *27*, 273.